

COMMUNICATION

Unravelling the key role of surface feature behind facet-dependent photocatalysis of anatase TiO₂

Received 00th January 20xx,
Accepted 00th January 20xx

DOI: 10.1039/x0xx00000x

Yung-Kang Peng,^{*a,b} Benedict Keeling,^a Yiyang Li,^a Jianwei Zheng,^a Tianyi Chen,^a Hung-Lung Chou,^c Tim J. Puchler,^d Robert A. Taylor^d and Shik Chi Edman Tsang^{*a}

It is commonly attributed the higher activity of nanocrystallite to its terminal high-energy facets. However, we demonstrate that high activity of anatase TiO₂ (001) facet in photocatalytic H₂ evolution is not due to its high intrinsic surface energy, but the local electronic effects created by surface features on the facet.

Tailoring surface of nanocrystallite with high-energy facets has recently attracted huge interests for a wide range applications as it in principle, leads to superior performance compared to that of enclosed by low-energy facets^{1–3}. However, as dictated by thermodynamics, it has never been an easy task to prepare nanocrystallite with high percentage of surface terminated by active facets. These high-energy facets grow faster and their exposure will be reduced during growth, resulting an equilibrium shape terminated with low-energy facets.¹ Accordingly, structure directing agents (SDA) that selectively anchor to metal atoms can effectively lower the overall surface energy and thus slow down the growth rate of high-energy facet relative to others. This stabilization is attributed to the generation of electric dipole between SDA and the metal atom that accompanies the modification of metal electronic structure on a particular facet.³ As a result, great effort has been made during the past decades to engineer terminal facets of nanocrystallites with high surface energy by kinetic shape control using selective adhesion of SDA.

Taking one of the most studied anatase TiO₂ as an example, the (001) facet (Scheme S1a) with intrinsically high surface energy (0.90 J m^{−2}) has often been claimed to be catalytically more active than the (101) facet (0.44 J m^{−2}) (Scheme S1b). However, it has been a challenge to experimentally prepare nanocrystallites with (001) facet at

high coverage^{9,10} to proof this point until a breakthrough was achieved by Yang et al. in 2008, using fluoride as a SDA to stabilize the (001) facet (form Ti–F) and hence reverses the relative thermodynamic stability of the two facets.¹¹ Since then, using fluoride as SDA to synthesize TiO₂ nanocrystals with various (001) coverages (via tuning hydrogen fluoride (HF) concentration) for the evaluation of facet-activity has been well-documented in photocatalysis,^{12–23} methanol conversion,²⁴ solar cell^{25,26} and lithium battery,²⁷ etc.

In general, removal of SDA after the morphology control is necessary to avoid its interference to the interested facet properties, especially in the field of heterogeneous (photo)catalysis associating the redox bonds breakage and formation at the catalyst surface. From thermodynamic point of view, upon the SDA removal, the uncapped high-energy facet must have experienced surface relaxation to minimize the increased system energy. According to our previous studies^{4–8}, the relaxation of high-energy facets may accompany with surface reconstruction to low-energy facets or/and the generation of surface features such as oxygen vacancy, hydroxyl group and cation/anion with various chemical states, mainly depending on post-treatments adopted for SDA removal.

However, literatures concerning anatase TiO₂ facet-dependent activity have often claimed to obtain a clean “Ti–O–Ti surface” of (001) facet (Scheme S1a) by a post-F removal via calcination at 600°C^{11–18,24–26} or ion exchange with aqueous NaOH^{13,14,19–23,28} regardless some additional surface features that might be generated and change their chemical states during the relaxation of (001) facets with the treated environments. As summarized and discussed in Table S1, nature of “facet” (i.e. difference in surface Ti_{5c} density between clean facets) or “surface feature” (i.e. surface fluorine or hydroxyl group) have been often attributed to be the principal factor to influence TiO₂ facet (photo)activity by different researchers even employing the same F removal method and catalytic reaction. To our point of view, the different interpretations even disagreements found among researchers could be attributed to the overlook of surface relaxation and the change of surface properties during post-treatments for later unambiguous correlation of facet activity.

^aThe Wolfson Catalysis Centre, Department of Chemistry, University of Oxford, Oxford, OX1 3QR, UK.

^bDepartment of Chemistry, City University of Hong Kong, Kowloon Tong, Hong Kong SAR, P. R. China.

^cGraduate Institute of Applied Science and Technology, National Taiwan University of Science and Technology, Taipei 10617, Taiwan.

^dClarendon Laboratory, Department of Physics, University of Oxford, Oxford, OX1 3PU, UK.

†Electronic Supplementary Information (ESI) available: Detailed preparation procedures of all TiO₂ particles, post-treatments, corresponding characterization and DFT calculation. See DOI: 10.1039/x0xx00000x

Herein, the surface features of TiO_2 crystallites are unravelled and quantified by probe-NMR technique for the investigation of their roles in photocatalytic H_2 activity. Surprisingly, the long-believed active (001) facet was found to play a negligible role in this reaction. Instead, the presence of SDA (i.e. fluorine) which can generate a local electronic effect significantly prolonging the excitons lifetime by the induced strong electric dipole ($\text{F}^{\delta-} \leftarrow \text{Ti}^{\delta+}$) at surface.

TiO_2 morphologies with different degrees of (001) coverage were firstly synthesized using HF as SDA during hydrothermal synthesis.^{11,19} Samples prepared with the addition of 0, 2 and 6 mL HF (50 wt%) show different shapes and are designated as OHF (Figure 1a), 2HF (Figure 1b) and 6HF (Figure 1c) with preferential exposed (101), (101)/(001) and (001) facets determined by subsurface TEM lattice spacing (Figure S1a-c) as often adopted in literature studying TiO_2 facet activity (Table S2).¹¹⁻²⁸ XRD analysis confirms that the three as-prepared TiO_2 samples all show the anatase crystal structure with similar crystallinity (Figure S2a). XPS F_{1s} signal in Figure S2b clearly increases with the HF added during hydrothermal synthesis in the order of 6HF > 2HF > OHF. To involve quantitative correlation of facet activity, the coverage of exposed (101) and (001) facets in each sample was further estimated according to Wulff construction (Figure S3) adopted in previous literature.^{11,19,27} As summarized in Figure S2c, the increase in HF concentration indeed brings an increase in face length (AB) and a reduction in thickness (AE) corresponding well to the reports in literature.¹¹ The area (coverage) of exposed (001) facet in each sample can be further calculated with corresponding Brunauer-Emmett-Teller (BET) surface area showing an increase from 12.6 m^2/g (10.2%) for OHF, 34.4 m^2/g (21.1%) for 2HF and 62.6 m^2/g (75.4%) for 6HF (Table S2).

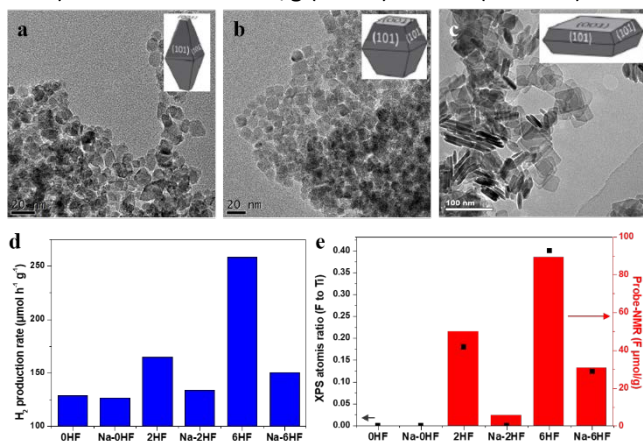


Figure 1. (a-c) TEM images of as-prepared (a) OHF, (b) 2HF, and (c) 6HF. (d) Photocatalytic hydrogen production rate (blue bar) of various faceted TiO_2 samples w/o NaOH wash and (e) their corresponding F concentration (red bar) determined by XPS atomic ratio and NMR (quantified by probe- ^{31}P NMR with signal at around 2 ppm, see below).

As stated, calcination treatment^{11-18,24-26} and NaOH wash^{13,14,19-23,28} are both often adopted for surface F removal before catalytic testing. The calcination removal of surface F is based on the hydrolysis of Ti-F into Ti-OH by H_2O in the flowing air at high temperature, while the NaOH wash is carried out via

a mild ion exchange (F^- and OH^-) in aqueous solution. However, from our characterization (Figures S4-S7) the calcination method is associated with the significant change of particle shape, size and hence (001) coverage. Also, the reconstruction of (001) facet to a more stable (1×4) (001) facet (Scheme S1c) during F removal at high temperature have been recently demonstrated by advanced TEM²⁹ and NMR⁵ techniques. Even though XPS result (Figure S6a-c) suggests the surface F can be completely removed at high temperature, these factors have unfortunately been ignored by those studies^{11-18,24-26} during their correlation of TiO_2 facet activity. In stark contrast, washing with NaOH doesn't seem to lead to major change in morphology (Figure S4d-f), crystallinity (Figure S4g-i), crystallite size and surface area (Figure S5) but a small amount of F residue on surface (Figure S6a-c)²⁸ that has been neglected in previous literature.^{13,14,19-23}

Accordingly, NaOH washed samples (denoted with prefix Na-) with maintenance of particle morphology/crystallinity and the surface area of (001)/(101) facets are adopted herein for the unbiased interrogation of the key role of surface feature in photocatalysis. As shown in Figure 1d, the photocatalytic H_2 production rates of 0/2/6HF samples are found in the order of 6HF > 2HF > OHF, which can directly correlate with their surface F contents (Figure 1e). Surprisingly, when surface fluorine is partly removed but keeping (001) exposure constant through the NaOH wash, a significant decrease in H_2 activity of both Na-2HF and Na-6HF but not for Na-OHF are observed. Noted that no common change of factor of a photocatalyst after NaOH wash such as surface area, crystallinity, bandgap and (001) coverage seems to meet this trend except the concentration of surface fluorine analysed by both XPS and NMR (Figure 1e) with the latter of higher sensitivity. This correlation can be supported by the fact that F-free OHF, Na-OHF and Na-2HF samples of similar total surface area ($\sim 140 \text{ m}^2/\text{g}$) all give H_2 activity around $125 \mu\text{mol h}^{-1} \text{g}^{-1}$. The OHF didn't experience any major change in activity after the NaOH wash (i.e. Na-OHF), implying the surface hydrolysis of Ti-O-Ti to Ti-OH has a very minor effect in this reaction. Also, considering that Na-2HF has similar surface area as both OHF and Na-OHF but has nearly tripled (001) exposure (34.4 m^2/g vs. 12.6 m^2/g , Table S2), the exposed (001) area should thus play a very minor role in the rate of H_2 production. Although the H_2 production rate of Na-6HF is much lower than that of 6HF, it remains higher in comparison to Na-OHF and Na-2HF. This is due to a considerable amount of F on its surface (Figure 1e) rather than its highest (001) exposure (62.6 m^2/g , Table S2).

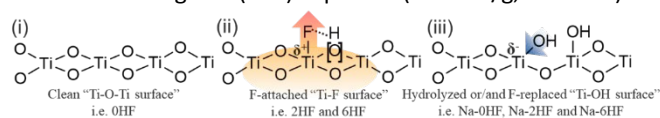


Figure 2. (a) Illustration on the change in surface function groups on TiO_2 facet: (i) initial clean "Ti-O-Ti surface", (ii) F-attached "Ti-F surface", (iii) hydrolyzed and F-replaced "Ti-OH surface" after NaOH wash.

As shown above, it is clearly that the concentration of surface fluorine rather than the long-believed (001) coverage plays the key role in photocatalytic H_2 production. However,

the local electronic effect induced by surface fluorine to TiO_2 remains largely unknown. Figure 2 shows the anticipated change of surface functional groups among samples induced by HF addition and NaOH wash. The OHF is supposed to expose clean (101) "Ti-O-Ti" facet (Figure 2(i)) while 2HF and 6HF expose different degrees of "F-attached" (001) facet (Figure 2(ii)). The post NaOH wash (Figure 2(iii)) can hydrolyze Ti-O-Ti to Ti-OH (for Na-OHF) and replace some Ti-F by Ti-OH (for Na-2HF and Na-6HF). To simplify the discussion, OHF, 6HF and Na-6HF were selected from each category to evaluate the electronic effect of fluorine and hydroxyl group imposed to TiO_2 surface. Considering the electron negativity of fluorine and hydroxyl group, the expected electron density of Ti atom on the top surface layer of TiO_2 is $\text{Ti-OH} > \text{Ti-O-Ti} > \text{Ti-F}$. However, no XPS chemical shift of both Ti_{2p} and O_{1s} (Figure S8) can be seen with the presence of surface F presumably due to the monitoring of core electrons of surface Ti and O makes XPS less sensitive to electronic effects from neighboring F atom(s). Also, XPS collects electrons from few atomic layers of the sample and is thus less sensitive to the electronic effect imposed by F to the top surface layer. Further attempt was carried out by Auger electron spectroscopy, which is believed to be more sensitive to the chemical environment compared to the core-level signals in XPS. Unfortunately, no distinguishable shift of Ti LMM and O KL1 Auger signals can be observed among samples (Figure S9). This suggests that the change of chemical state of surface Ti is still diluted from subsurface Ti sites due to the long electron escape depth of both techniques. This might explain why literature has often assumed no catalytic effect of fluorine when correlating TiO_2 facet activity in the past decade.¹¹⁻²⁸

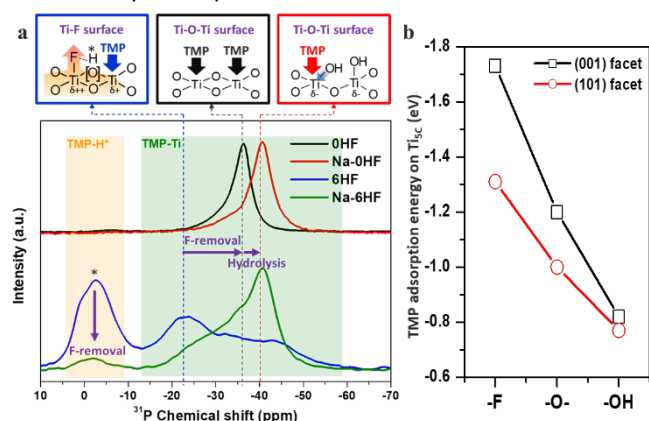


Figure 3. (a) TMP-assisted ^{31}P NMR spectra of OHF and 6HF w/o NaOH wash (orange area: interaction between TMP and acidic proton induced by F*; green area: interaction between TMP and surface unsaturated Ti). (b) The calculated adsorption energies (E_{ad}) of TMP to Ti_{5c} on (001) and (101) facets with surface -F, -O- and -OH group.

Very recently, we have developed an advanced technique for the surface investigation of faceted metal oxide using probe molecule (i.e. trimethylphosphine, TMP) assisted solid-state ^{31}P NMR.⁴ It was shown that the ^{31}P chemical shift ($\delta^{31}\text{P}$) of the TMP-metal adduct can differentiate the surface metal cations between various chemical states at high resolution through Lewis acid-base interaction ($\delta^{31}\text{P}$: -20 ~ -60 ppm,

green area in Figure 3a). Metal cation with strong acid strength can generate stronger bond with TMP and thus pushes $\delta^{31}\text{P}$ to downfield (shift to positive ppm). On the other hand, the interaction between TMP and acidic hydroxyl proton will give a signal at $\delta^{31}\text{P}$ around -2 ppm (orange area in Figure 3a). Figure 3a shows TMP- ^{31}P NMR results of OHF and 6HF samples w/o NaOH wash. The evolution of signal at -2 ppm of 6HF (blue line) suggests the generation of acidic proton due to the stabilization of hydrogen by surface F while no such signal can be observed for F-free OHF (black line). In addition, a significant negative shift from -22 ppm for 6HF to -36 ppm for F-free OHF indicates the electron density of surface Ti_{5c} is largely decreased with the presence of F. Noted that for 6HF sample the electronic effect imposed by F is sensitized by TMP on the secondary Ti_{5c} (cf. primary Ti_{5c} for OHF). The electron density of its primary Ti_{5c} (can not be probed by TMP) of strongly polarized Ti-F is thus expected much lower. In stark contrast, the electronic effect induced by hydrolysis (NaOH wash) on clean surface is very minor that only a tiny $\delta^{31}\text{P}$ shift from -36 ppm (for OHF, black line) to -41 ppm (for Na-OHF, red line) can be observed. This results can be further supported by Na-6HF sample (green line) that NaOH wash has largely decreased the signal intensity at -2 ppm and also re-distributed $\delta^{31}\text{P}$ between -20 ~ -60 ppm due to the co-presence of residue Ti-F and Ti-OH on surface.

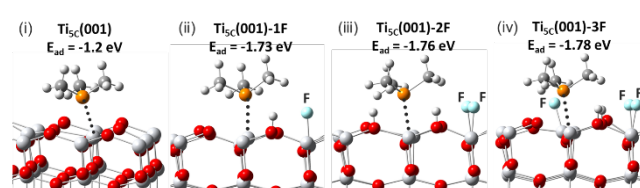


Figure 4. Schematic illustration of TMP adsorbed Ti_{5c} on (001) facet (i) without F and promoted with (ii) 1F, (iii) 2F, (iv) 3F atoms (P: orange; C: light grey; H: white; F: cyan).

As seen from the calculated adsorption energies (E_{ad}) of TMP to Ti_{5c} on functionalized (001) and (101) facets (Figure 3b), the presence of F surface can largely enhance the TMP adsorption energy to surface Ti_{5c} by surface polarization on both facets (cf. Ti-O-Ti and Ti-OH) whereas only 0.05 eV difference between facets when they are both hydroxylated.

On the other hand, the increasing calculated E_{ad} of TMP probe on surface Ti_{5c} at higher F coverage on (001) surface (Figure 4) can further reflect the progressive enhancement in local surface polarization effect. This may explain why the catalytic activity of the (001) facet observed experimentally should be closely associated with surface attached F that polarize the exposed surface Ti, while hydroxylated (101) and (001) surfaces exhibit similar activity (i.e. OHF, Na-OHF and Na-2HF in Figure 1d).

When excited photogenerated holes and electrons in this semiconductor oxide are generated during photocatalysis, the holes and electrons can be polarized immediately by such local electric field induced by the surface F. Since water/methanol adsorption on catalyst' surface is not the rate-determining step in H_2 production due to the solvation of catalysts, the key factor should be relevant to the change of physiochemical

properties on TiO₂ surface imposed by SDA. The role of surface F in photocatalytic H₂ evolution was then investigated by time-resolved photoluminescence (TRPL), as the better local exciton separation at surface could benefit to the photocatalytic activity. It should be noted that all faceted TiO₂ samples were hydrothermally prepared at 180°C with similar crystallinity and both -F and -OH were attached onto the particles' top surface where the reaction is taken place. Accordingly, the exciton lifetime should closely associate with the element introduced onto the particles' top surface layer. It is clear from the TRPL plots (Figure S10) and corresponding fitting results (Table S4) that both f1 and f2 components and corresponding averaged lifetime (τ_{avg}) increase along with the concentration of surface fluorine from 0HF to 2HF to 6HF. The role of fluorine in prolonging exciton lifetime can be further supported by the decrease of f2 component (4.55 ns to 3.60 ns) and averaged lifetime (3.96 ns to 2.55 ns) observed when 6HF sample was further washed with NaOH. The increased f1 component of Na-6HF is unclear presumably due to the co-existence of abundant Ti-F and Ti-OH on surface. Clearly, fluorine in the strongly polarized F^{δ-}—Ti^{δ+} bond (the only bond stronger than Ti-O bond¹¹) reduces the recombination rate of photogenerated electrons and holes by acting as a surface electron-trapping site to trap the photogenerated electrons due to its strongest electronegativity,³ and hence increases photoactivity. We believe the effect of fluorine imposed on the surface exciton lifetime should be more pronounced than the observed lifetime in Table S4 considering TRPL is a technique collecting signal from both surface and bulk.

The deposition of Pt nanoparticles by UV-assisted wet impregnation onto TiO₂ surfaces as co-catalyst has been widely adopted during the evaluation of TiO₂ facet-dependent H₂ activity. A recent calculation showed that the H₂ production rate is highly associated with Pt loading and its size on TiO₂,³⁰ however, the surface F effect on the loading of photo-reduced Pt nanoparticles has often been overlooked by those studies when investigating facet activity. As shown in Figure S11 and S12, both the loading and size of Pt nanoparticles highly associate with the concentration of surface fluorine rather than the exposed facet due to the facilitated photo-deposition by the extended exciton lifetime. The influence of surface fluorine in photoreaction is again proved to play a more important role than the high-energy (001) facet.

In conclusion, our results clearly suggest that the higher surface energy of (001) facet than (101) facet does not seem to play a dictating role in affecting photocatalytic H₂ production rate from water as that claimed in literature. We attribute the dominate rate altering effect to the local electronic modification imposed by surface F as stabilizer, which unfortunately cannot be easily removed from (001) TiO₂ without facet reconstruction or/and the generation of surface features. Our results also suggest that the reactivity of hydroxylated (001) and (101) facets are similar to each other despite the fact that the clean (001) facet is reported in higher energy than the latter.

The authors would like to thank the EPSRC research council of UK for funding support. The work described in this paper

was also supported by a grant from City University of Hong Kong (Project No. 7200584 and Project No. 9610415).

Conflicts of interest

The authors declare no competing financial interest.

Notes and references

- Y. Yin, A. P. Alivisatos, A. P. *Nature* **2005**, *437*, 664.
- T. E. Madey, W. Chen, H. Wang, P. Kaghazchi, T. Jacob, *Chem. Soc. Rev.* **2008**, *37*, 2310.
- M. A. Boles, D. Ling, T. Hyeon, D. V. Talapin, *Nat. Mater.* **2016**, *15*, 141.
- Y.-K. Peng, L. Ye, J. Qu, L. Zhang, Y. Fu, I. F. Teixeira, I. J. McPherson, H. He, S. C. E. Tsang, *J. Am. Chem. Soc.* **2016**, *138*, 2225.
- Y.-K. Peng, Y. Hu, H.-L. Chou, Y. Fu, I. F. Teixeira, L. Zhang, H. He, S. C. E. Tsang, *Nat. Commun.* **2017**, *8*, 675.
- Y.-K. Peng, Y. Fu, L. Zhang, I. F. Teixeira, L. Ye, H. He, S. C. E. Tsang, *ChemCatChem* **2017**, *9*, 155.
- Y.-K. Peng, H.-L. Chou, S. C. E. Tsang, *Chem. Sci.* **2018**, *9*, 2493.
- Y.-K. Peng, S. C. E. Tsang, *Nano Today* **2018**, *18*, 15.
- S. Liu, J. Yu, M. Jaroniec, *Chem. Mater.* **2011**, *23*, 4085.
- G. Liu, H. G. Yang, J. Pan, Y. Q. Yang, G. Q. Lu, H.-M. Cheng, *Chem. Rev.* **2014**, *114*, 9559–9612.
- H. G. Yang, C. H. Sun, S. Z. Qiao, J. Zou, G. Liu, S. C. Smith, H. M. Cheng, G. Q. Lu, *Nature* **2008**, *453*, 638.
- H. G. Yang, G. Liu, S. Z. Qiao, C. H. Sun, Y. G. Jin, S. C. Smith, J. Zou, H. M. Cheng, G. Q. Lu, *J. Am. Chem. Soc.* **2009**, *131*, 4078.
- S. Liu, J. Yu, M. Jaroniec, *J. Am. Chem. Soc.* **2010**, *132*, 11914.
- Q. Xiang, K. Lv, J. Yua, *Appl. Catal. B* **2010**, *95*, 557.
- J. Pan, G. Liu, G. Q. Lu, H.-M. Cheng, *Angew. Chem. Int. Ed.* **2011**, *50*, 2133.
- T. Tachikawa, S. Yamashita, T. Majima, *J. Am. Chem. Soc.* **2011**, *133*, 7197.
- Q. Wu, M. Liu, Z. Wu, Y. Li, L. Piao, *J. Phys. Chem. C* **2012**, *16*, 26800.
- J. Yu, J. Low, W. Xiao, P. Zhou, M. Jaroniec, *J. Am. Chem. Soc.* **2014**, *136*, 8839.
- X. Han, Q. Kuang, M. Jin, Z. Xie, L. Zheng, *J. Am. Chem. Soc.* **2009**, *131*, 3152.
- J. Yu, L. Qi, M. Jaroniec, *J. Phys. Chem. C* **2010**, *114*, 13118.
- T. R. Gordon, M. Cargnello, T. Paik, F. Mangolini, R. T. Weber, P. Fornasiero, C. B. Murray, *J. Am. Chem. Soc.* **2012**, *134*, 6751.
- Y. Luan, L. Jing, Y. Xie, X. Sun, Y. Feng, H. Fu, *ACS Catal.* **2013**, *3*, 1378.
- X. Yu, B. Jeon, Y. K. Kim, *ACS Catal.* **2015**, *5*, 3316.
- F. Xiong, Y.-Y. Yu, Z. Wu, G. Sun, L. Ding, Y. Jin, X.-Q. Gong, W. Huang, *Angew. Chem. Int. Ed.* **2016**, *55*, 623.
- X. Wu, Z. Chen, G. Q. Lu, L. Wang, *Adv. Funct. Mater.* **2011**, *21*, 4167.
- L. Chu, Z. Qin, J. Yang, X. Li, *Sci. Rep.* **2015**, *5*, 12143.
- J. S. Chen, Y. L. Tan, C. M. Li, Y. L. Cheah, D. Luan, S. Madhavi, F. Y. C. Boey, L. A. Archer, X. W. Lou, *J. Am. Chem. Soc.* **2010**, *132*, 6124.
- G. Jeantelot, S. Ould-Chikh, J. Sofack-Kreutzer, E. Abou-Hamad, D. H. Anjum, S. Lopatin, M. Harb, L. Cavallo, J.-M. Basset, *Phys. Chem. Chem. Phys.* **2018**, *20*, 14362.
- W. Yuan, Y. Wang, H. Li, H. Wu, Z. Zhang, A. Selloni, C. Sun, *Nano. Lett.* **2016**, *16*, 132.
- D. Wang, Z.-P. Liu, W.-M. Yang, *ACS Catal.* **2018**, *8*, 7270.